nature physics

SUPPLEMENTARY INFORMATION

DOI: 10.1038/NPHYS1765

Zernike Phase Contrast in Scanning Microscopy with X-rays

- Supplementary Information -

Christian Holzner,[1,*] Michael Feser,[2] Stefan Vogt,[3] Benjamin Hornberger,[2] Stephen B. Baines,[4] and Chris Jacobsen,[1]

[1] *Department of Physics and Astronomy, Stony Brook University, Nicolls Road, Stony Brook, NY 11794, United States*

[2] *Xradia Inc., 5052 Commercial Circle, Concord, CA 94520, United States*

[3] *Advanced Photon Source, Argonne National Laboratory, 9700 S Cass Avenue, Argonne, IL 60439, Unites States*

[4] *Department of Ecology and Evolution, Stony Brook University, Nicolls Road, Stony Brook, NY 11794, United States*

[*] *To whom correspondence should be addressed: cholzner@xray1.physics.sunysb.edu*

I. EXPERIMENTAL DETAILS

Experiments were performed at the sector 2 insertion device side branch beamline 2-ID-E at the Advanced Photon Source, Argonne National Laboratory [1]. X-rays from an undulator source were energy filtered via a Si(111) crystal monochromator. An additional beam splitting crystal was used to reflect part of the main beam into the side branch line. The existing scanning fluorescence setup was modified to accommodate the additional optical elements and realize the detector geometry. A schematic of all the optical components used at the experimental end station for the experiment described is shown in Suppl. Fig. 1a. The x-ray energy chosen for the experiment was 10 keV, which is a typical energy used for trace element mapping for life science. The 10 keV X-rays were focused using a 160 μm diameter Fresnel zone plate with outermost zone width of 100 nm and zone height of 1600 nm; an arrangement of 40 μm diameter central stop (approx. 80 μm thick gold) and 25 μm diameter order sorting aperture was used to isolate the first order focus of the zone plate. A phase ring made of gold with a thickness of 3.52 μm and 75 μm inner and 85 μm outer diameter was placed 151 mm upstream of the zone plate.

The samples were placed in the focal plane of the zone plate and raster scanned through the focus spot of the lens. A fluorescence detector (not shown in schematic) was placed under 90° to the optical axis to minimize the elastic scattering background and directly pointed at the focal spot of the x-rays on the sample. In order to avoid shadowing of the fluorescence through the sample holder, the sample stage is rotated by 15° around the vertical axis.

DOI: 10.1038/NPHYS1765

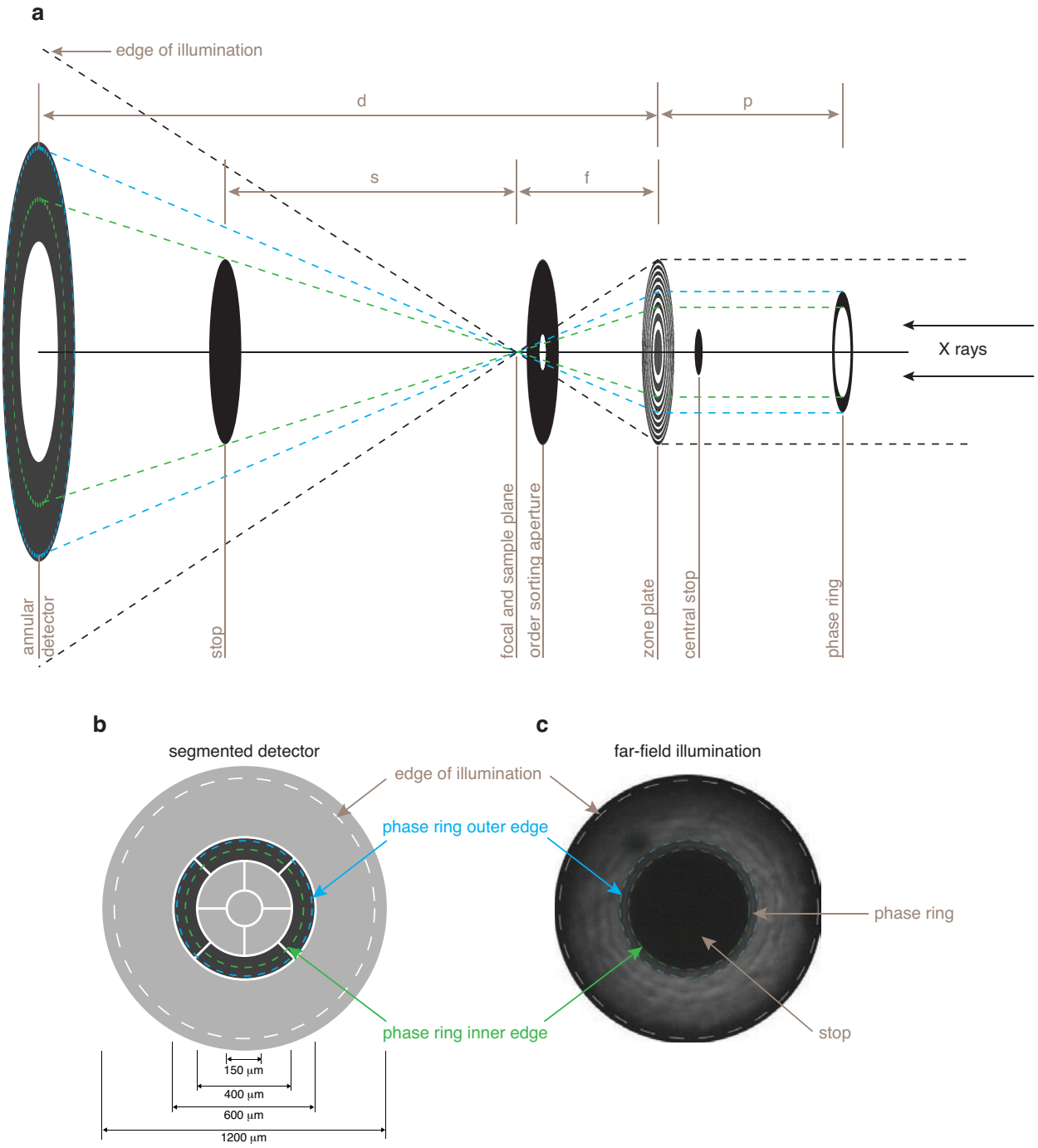

SUPPL. FIG. 1: **a** Arrangement of the optical components used in the experiment (not to scale). **b** Schematic of the 10-segment detector, the four segments that were used to realize the annular detector are highlighted; boundaries between the segments are exaggerated. **c** Far-field illumination recorded with a CCD in place of the segmented detector. In all three panels of the figure the inner and outer edge of the phase ring are inidicated by green and blue respectively. Both b and c are of true relative scale.

An annular detector was used in the far-field to record the projection of the phase ring. The annular detector was realized through an existing 10-segment detector [2]; Suppl. Fig. 1b shows a schematic, highlighting the four segments that were used to make up the annular detector. In Suppl. Fig. 1c an image of the far-field illumination pattern recorded with a scintillator-coupled CCD in place of the segmented detector is shown. Both Suppl. Fig. 1b and 1c are of true relative scale and illustrate how the detector was aligned to the illumination pattern: the outer edge of the phase ring projection was matched with the outer edge of the annular quadrant. Since the phase rings projection was much smaller than the annular detector (see Suppl. Fig. 1b, phase ring inner edge) an additional stop was put in front of the detector to mask it optimally to the projection of the phase ring and, therefore, eliminating the detection of unwanted signal. The stop with a diameter of 160 μm was put at a distance (s = 280 mm) from the sample, so as to have its diameter match the inner diameter of the phase rings projection in this plane (see Suppl. Fig. 1a).

A scanning Zernike image represents the signal of the annular detector at each raster scan point. Unless otherwise noted, each image was recorded with a step size of 100 nm and a dwell time per raster point of 100 ms. Absorption images were taken by performing a separate scan, where the phase ring and stop were removed from the setup. In this case the sum of all 10 detector segments represents the absorption image.

Given the focal length ($f = 131$ mm) of the zone plate and the necessary distance of the detector to the zone plate ($d = 1031$ mm) to align the outer edge of the phase ring with the annular detector, the position of the phase ring in front of the zone plate ($p = 151$ mm) was chosen to fulfill the lens equation $1/p + 1/d = 1/f$. Note, that the ideal detector to zone plate distance would have been $d = 1056$ mm; however, d was chosen smaller to allow some tolerance for small errors in alignment. Furthermore, tests were performed where the phase ring was brought significantly closer (up to $p = 50$ mm) or further away (up to $p = 250$ mm) from its ideal position; however, no noticeable differences in the imaging results were observed. The relaxed positioning tolerance is associated with the fact that we are dealing with an almost planar incident wave front (rays close to parallel to the optical axis) upstream of the objective lens, attributed to a source more than 15 m away. As a consequence the rays that pass through the phase ring will hit the detector correctly regardless of the phase ring position along the optical axis. In the full-field imaging case the phase ring position is much more restricted due to a stronger converging wave field.

DOI: 10.1038/NPHYS1765

II. EQUIVALENCE OF SCANNING TO FULL-FIELD ZERNIKE PHASE CONTRAST

Theoretically and mathematically, both cases are completely equivalent. A minor technical difference for X-rays will be the requirement of a central stop (CS) in the objective pupil for scanning, which is not needed in the full-field case. The CS modifies the shape of the modulation transfer function of the lens to some degree. This difference has no disadvantageous effects and is of a rather technical nature. Note however, that the complete equivalence only applies to on-axis image points. Mathematical differences will arise for image points that are far away from the optical axis in full-field imaging; scanned imaging is always on-axis by default. Furthermore, it is very likely that there will be differences for very extreme imaging cases in terms of very strong absorbing and phase shifting objects. Differences in the case of dark field (infinitely thick phase ring) imaging are difficult to predict due to the non-linear and higher order nature of this imaging mode. These aspects are beyond the scope of our work, but pose interesting questions for future publications.

III. SCANNING ZERNIKE IMAGES OF TEST STRUCTURES

In Suppl. Fig. 2a we show a scanning Zernike image of a pair of 5 μm diameter polystyrene spheres imaged at 10 keV. A bright halo artifact, which is typical for Zernike phase contrast, can be seen around the edges of the two spheres. Another artifact common for this imaging method is illustrated by the line-out through the left sphere in the image (Suppl. Fig. 2b). Rather than decreasing to a minimum towards the center of the sphere (indicated by the arrow), we note an increase in the image intensity. Both artifacts, which are due to the nature of how the contrast is formed (ring shaped phase mask and aperture), are typical for Zernike phase contrast images and are a consequence of the loss of low spatial frequencies in the image formation process. While such artifacts are not desired, here they further demonstrate the equivalence of the presented scanning Zernike phase contrast and the full-field case.

A further demonstration of the techniques imaging properties is given through Suppl. Fig. 3, which shows the scanning Zernike image (Suppl. Fig. 3a) of a plastic zone plate structure. The corresponding absorption image (Suppl. Fig. 3b) of a subregion has no contrast. In the profile through the first column of the scanning Zernike image a decrease in contrast with feature size can be observed, confirming the imaging behavior as one would expect them from such an incoherent imaging system.

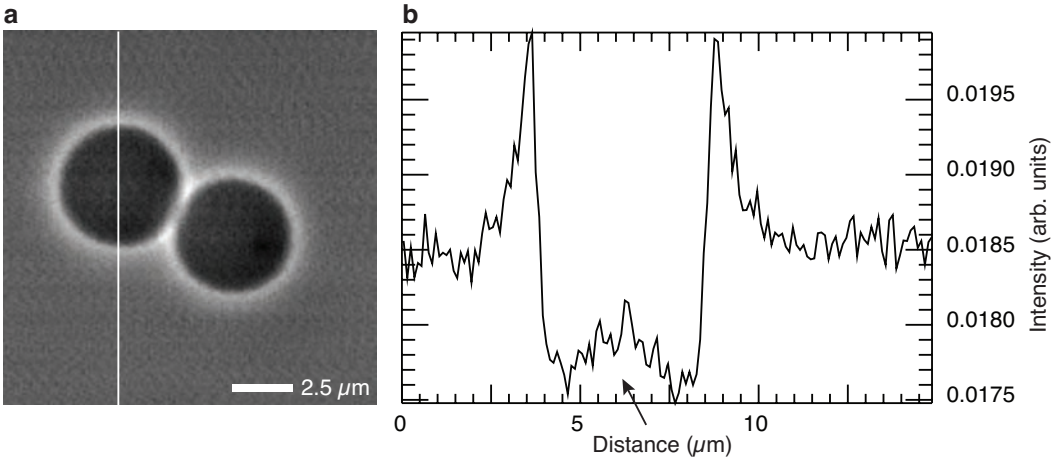

SUPPL. FIG. 2: **a** Scanning Zernike phase contrast image of a pair polystyrene spheres with a diameter of 5 m. **b** Profile through the left sphere as indicated in a by the vertical line. The arrow points to the approximate center of the sphere.

IV. REMOVAL OF THE PHASE RING

To further illustrate the scanning Zernike imaging properties we investigate the effects when the phase ring is removed from the setup. Supplementary Fig. 4a shows the same pair of polystyrene spheres from Suppl. Fig. 2, again in scanning Zernike phase contrast and also with the phase ring taken out (Suppl. Fig. 4b). A clear difference is noticeable; only the outlines of the spheres with their edges are visible in the case without the phase ring. Note, that there is no noticeable contrast to the sphere interior. Line profiles through both images are shown in Suppl. Fig. 4c.

[1] J. Maser, D. Legnini, S. Vogt, Z. Cai, and B. Lai (2001), unpublished.

[2] B. Hornberger, M. D. de Jonge, M. Feser, P. Holl, C. Holzner, C. Jacobsen, D. Legnini, D. Paterson, P. Rehak, L. Strüder, et al., Journal of Synchrotron Radiation **15**, 355 (2008).

DOI: 10.1038/NPHYS1765

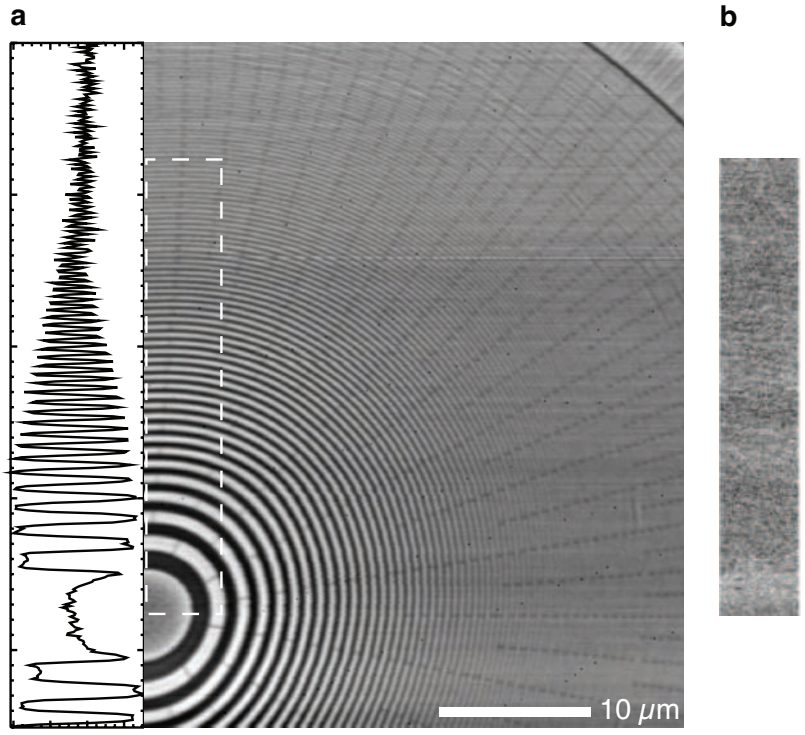

SUPPL. FIG. 3: **a** Scanning Zernike image of a plastic zone plate test structure; also shown is a line-out through the first image column. **b** Absorption image of the region indicated in the Zernike image.

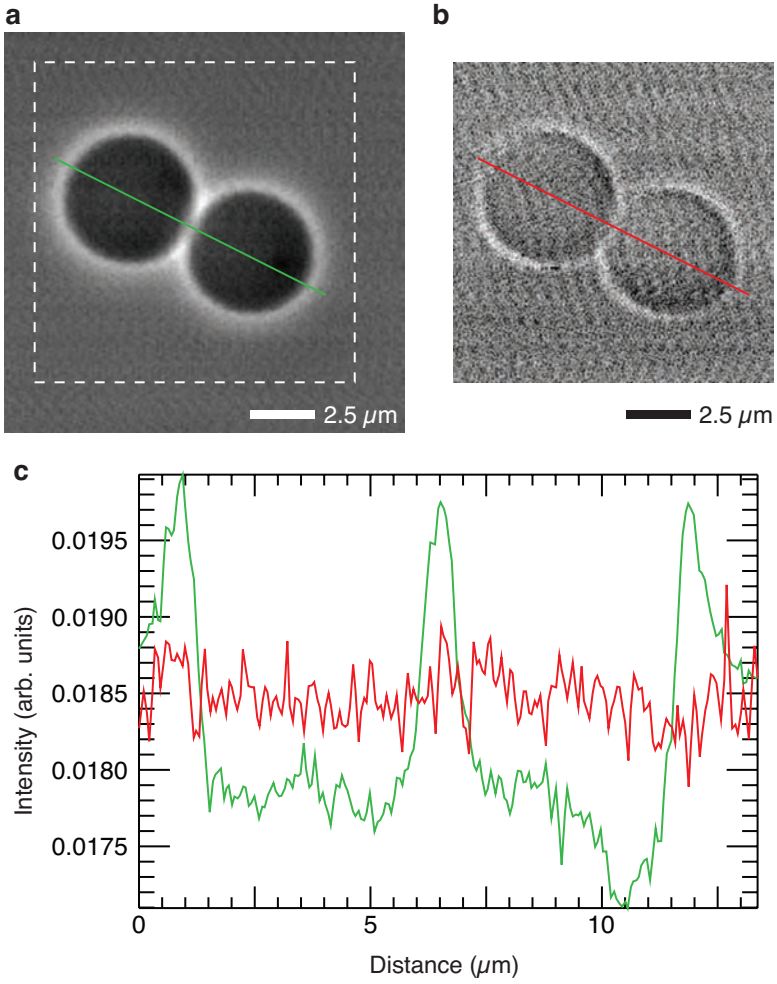

SUPPL. FIG. 4: **a** Scanning Zernike image from a pair of polystyrene spheres (identical to Suppl. Fig. 2a); **b** same pair of spheres imaged with the phase ring removed from the setup, the scan area is identified in a with a dashed box. **c** Line profiles through a (red) and b (green) as indicated in the images. (Note: b was imaged with a 50 nm step size, the image was linearly scaled down to match a, which had a step size of 100 nm.)